

Rapidity characteristics at cosmic-ray energies

R. K. Shivpuri and Chandra Gupta

Department of Physics and Astrophysics, University of Delhi, Delhi-110007, India

Tara Chand

Department of Physics, St. Stephens College, University of Delhi, Delhi-110007, India

Triyug Singh

Department of Physics, Shivaji College, University of Delhi, Delhi-110007, India

(Received 24 December 1974; revised manuscript received 12 February 1976)

The various characteristics of rapidity of secondary particles in interactions at cosmic-ray energies ($\sim 10^{12}$ eV) have been investigated. The features studied are the dependence of maximum-rapidity-gap value on primary energy and multiplicity, the rapidity-difference distribution, and the rapidity distribution of the secondary particles. The results have been compared with the predictions of the multiperipheral model.

I. INTRODUCTION

Ever since the concept of rapidity was introduced by Feynman,¹ a number of investigations have been carried out to explain various experimental observations in terms of this parameter. There are a number of advantages in understanding the interaction mechanism in terms of rapidity rather than the simple longitudinal momentum (P_L) distribution or a Peyrou plot (P_L vs P_T). The rapidity distribution for low values has a wide dispersal and exhibits a regularity which is independent of the primary energy; there is complete symmetry between the laboratory and projectile frames.

Although very high center-of-mass energies are presently obtained at Fermilab and CERN ISR, cosmic rays continue to be the source of the highest available energy. Hence it would be quite valuable to get a deeper insight into the various experimental features at cosmic ray energies—particularly in the TeV region. We present below the first experimental characteristics of rapidity in nucleon-nucleon interactions at ultrahigh energies ($\sim 10^{12}$ eV) and compare them with those at 205 GeV/c p - p collisions.

The two processes which dominate the hadronic cross section at high energies are the diffractive and nondiffractive components. Recently, Jones and Snider² suggested the usage of maximum rapidity gap (Δ) between adjacent particles as a means of determining the contribution of diffractive dissociation (Pomeron exchange) in the interactions. The merit of using the maximum-rapidity-gap variable is that it offers an energy-independent method of determining the contribution of diffractive dissociation in the data. Such an analysis can be carried out event by event for the same incident energy. A diffractive event² is one where one (or both) of incident particles fragments into

particles having, in aggregate, the same quantum numbers as the incident particle. Hence, in such an event there is a Pomeron exchange which leads to large subenergies and hence to large gaps in rapidity. From an experimental point of view, the approach suggested by Jones and Snider² is simple and attractive enough to investigate if the observed value of Δ could be used as a determining factor to separate the contribution from diffractive and nondiffractive components at cosmic ray energies. We find that the Δ spectrum for low- and high-multiplicity events overlaps for a majority of events, but there tends to be a greater contribution to large Δ values from low-multiplicity events than from high-multiplicity events. The observed mean value of the maximum rapidity gap exhibits an increase with decreasing mean multiplicity of the interactions. It has been shown that at the primary energies of the interactions in the range of 0.1–2600.0 TeV, the maximum-rapidity-gap value does not show any dependence upon primary energy.

In an interesting work, Snider³ has proposed a multiperipheral model which describes the two-charged-particle correlations and the rapidity-gap distributions for the nondiffractive component of the total cross section at 205 GeV/c. We compare the results of Snider³ with the present work on rapidity-gap distribution in the central plateau at primary energies greater than 1 TeV. Lastly we show that the rapidity distributions approach energy-independent limits in agreement with the multiperipheral model.

At high energies the Lorentz-contracted field of a nucleon is so sharp along the direction of motion that the energy in it is distributed uniformly in longitudinal momentum. The longitudinal-momentum distribution of the secondary particles follows the form dP_L/E , where E is the energy of

the secondary particle.

Writing the rapidity as,

$$dy = \frac{dP_L}{E}, \quad (1)$$

$$y = \frac{1}{2} \ln \left(\frac{E + P_L}{E - P_L} \right). \quad (2)$$

At cosmic-ray energies it can be assumed that $P_L \gg P_T \gg m$, where P_T and m denote the transverse momentum and mass of the secondary particles, respectively.

Hence, we get from Eq. (2)

$$y = \ln \left(\frac{2}{\tan \theta} \right), \quad (3)$$

where θ is the laboratory angle of the secondary particle. The experimental data used here are taken from the ICEF data sheet⁴ and the following criteria were adopted to select the events.

(1) The primary energy (E_p) of the interaction must be greater than 0.1 TeV.

(2) The number of low-energy particles⁵ (heavy tracks, n_h) should be equal to zero. This criterion was followed in order to ensure that there is no momentum transfer to the nucleus and that the collision is effectively a nucleon-nucleon type.

The number of events satisfying the above criteria was found to be 36. The data for 16 nucleon-nucleon interactions from the Chicago stack reported earlier⁶ has also been considered in the present analysis. Thus the total number of events is 52, yielding the number of secondary particles equal to 801. In Table I is given the event type, the primary energy, and the rapidity values of secondary particles for each event. The interactions considered here are the semi-inclusive processes since the rapidities of only the charged particles are determined.

II. RESULTS AND DISCUSSION

A. Variation of maximum-rapidity-gap value with primary energy

The values of the rapidities of all the secondary particles in an event were calculated using Eq. (3). The rapidity difference between adjacent particles in an event was determined; Δ was the maximum value of rapidity difference in the secondary particles of an interaction. The value of primary energy in an interaction was determined by using the following formula of Castagnoli *et al.*⁷

$$\log \gamma_c = \frac{1}{n_s} \langle \log \cot \theta \rangle, \quad (4)$$

where $\gamma_c = 1/(1 - \beta_c^2)^{1/2}$, β_c is the velocity of the center of mass, and n_s (Ref. 5) is the multiplicity

of the charged secondary particles in an event. The value of primary energy was found from the relation

$$E_p = M_n (2\gamma_c^2 - 1),$$

where M_n is the nucleon mass. The contribution of the persisting primary in an interaction was not considered in the determination of γ_c as it is not a secondary particle, and this procedure leads to a better estimate of the primary energy.⁸ The primary energy of the interactions range from 0.1 to 2600.0 TeV. Figure 1 shows the maximum-rapidity-gap value plotted against the corresponding primary energy of an interaction. It is clear that no dependence of Δ on primary energy is observed. The energy-independent characteristic of Δ makes it a useful parameter for understanding the interaction mechanism.

B. Variation of maximum rapidity gap with multiplicity

In order to determine if the magnitude of the maximum rapidity gap can be used to separate the contribution from diffractive and nondiffractive dissociations, the distribution of Δ and its variation with multiplicity has been studied. Figure 2 shows the variation of the mean value of Δ plotted against the mean multiplicity. The general trend of the distribution shows that as the mean multiplicity decreases, the mean value of Δ increases. This can be explained by a reasonable assumption that the low-multiplicity events have larger sub-energies than the high-multiplicity events, and hence the former should have larger values of Δ than the latter. The low-multiplicity events are dominated by diffractive dissociation (Pomeron exchange) and hence should lead to high values of Δ . The broad spread of the points in Fig. 2 is probably due to (i) the different primary energies of the interactions, which lead to different values of multiplicity and also (ii) the likely contribution of low-multiplicity events in nondiffractive regions and of high-multiplicity events in diffractive regions.

From the Δ distribution of events having all multiplicities it is not possible to determine the contribution of the diffractive and nondiffractive dissociations. The contributions to Δ from low- and high-multiplicity events overlap to a considerable extent. The overlapping could be due to an appreciable number of Pomeron-exchange events in the nondiffractive regions. Jones and Snider² have investigated the Δ distribution on the basis of the multiperipheral model and have shown that the primary energy of 205 GeV/c is not sufficient to separate the contribution from diffractive and non-

TABLE I. The event type, primary energy, and rapidity values of secondary particles are given for each event. [The first 36 events are from the ICEF data (Ref. 4) and the other 16 events are from the Chicago stack (Ref. 6).] The underlined values of rapidity for each event are at the two ends of the rapidity space. The absence of one underlined rapidity value in an event means that the angle of the leading primary particle was not measured.

Serial number	Event type	Primary energy (TeV)	Rapidity values
1	0+36p	644.52	<u>3.04</u> , 3.27, 4.21, 4.47, 5.11, 5.11, 5.11, 5.28, 6.65, 7.07, 7.07, 7.39, 7.39, 7.39, 7.46, 7.53, 7.64, 7.64, 7.71, 7.71, 7.78, 7.83, 7.88, 7.97, 8.01, 8.04, 8.11, 8.24, 8.24, 8.36, 8.36, 8.36, 8.47, 8.52, 8.61, <u>8.80</u> .
2	0+16p	0.24	<u>1.68</u> , 1.80, 2.72, 2.77, 2.79, 2.79, 3.04, 3.13, 3.20, 3.29, 3.68, 3.80, 3.89, 3.98, 4.10, <u>4.24</u> .
3	0+9p	70.34	<u>4.90</u> , 5.11, 5.32, 5.48, 5.48, 6.38, 7.12, 7.88, <u>7.88</u> .
4	0+9n	0.57	<u>1.89</u> , 2.10, 2.28, 2.72, 3.38, 4.81, 5.43, 5.80, <u>5.99</u> .
5	0+22p	16.19	<u>0.96</u> , 2.53, 4.03, 4.08, 4.26, 4.51, 4.63, 4.79, 5.57, 5.64, 5.69, 5.78, 6.01, 6.06, 6.06, 6.08, 6.19, 6.38, 6.40, 6.45, 7.60, <u>7.62</u> .
6	0+8p	1.04	<u>2.62</u> , 2.69, 3.06, 3.89, 3.94, 5.32, 5.43, <u>6.26</u> .
7	0+13n	1.77	<u>1.93</u> , 2.90, 2.97, 3.43, 3.91, 4.19, 4.21, 4.61, 4.88, 5.92, 6.33.
8	0+30n,p	3.09	<u>2.39</u> , 2.49, 2.97, 3.06, 3.38, 3.38, 3.45, 3.48, 3.50, 3.85, 3.85, 3.85, 3.94, 3.96, 4.12, 4.14, 4.21, 4.28, 4.37, 4.47, 4.65, 5.09, 5.11, 5.53, 5.87, 5.92, 6.19, 7.30, 7.30, <u>7.30</u> .
9	0+16p	3.69	<u>2.44</u> , 2.97, 3.50, 3.57, 3.68, 4.05, 4.54, 4.54, 4.61, 4.77, 5.07, 5.71, 5.80, 5.94, 6.08, <u>6.08</u> .
10	0+11p	0.17	<u>1.66</u> , 2.49, 2.53, 2.65, 2.67, 2.67, 3.57, 3.57, 3.73, 3.91, <u>3.91</u> .
11	0+14n	0.51	<u>0.64</u> , 1.08, 2.04, 2.26, 2.28, 2.53, 3.80, 4.10, 4.93, 4.93, 5.02, 5.48, 6.38.
12	0+9p	0.33	<u>1.89</u> , 2.49, 2.79, 3.02, 3.18, 3.64, 4.05, 5.16, <u>5.48</u> .
13	0+9p	2.62	<u>2.49</u> , 3.62, 4.49, 4.56, 4.70, 4.79, 4.83, 5.02.
14	0+13p	7.68	<u>0.39</u> , 2.95, 3.82, 4.10, 4.70, 4.86, 5.66, 5.99, 6.24, 6.38, 6.56, 6.56, <u>6.65</u> .
15	0+10p	21.74	<u>4.79</u> , 5.16, 5.20, 5.20, 5.32, 5.50, 5.57, 5.76, 5.83, <u>6.27</u> .
16	0+13p	0.87	<u>1.73</u> , 3.18, 3.87, 3.87, 3.91, 3.91, 4.03, 4.10, 4.12, 4.12, 4.14, 4.14, <u>4.21</u> .
17	0+15p	1.13	<u>1.13</u> , 1.29, 1.64, 1.73, 2.02, 2.99, 4.37, 5.09, 5.20, 5.37, 5.87, 5.87, 5.92, 5.99, <u>7.02</u> .
18	0+18p	0.47	<u>2.14</u> , 2.28, 3.11, 3.22, 3.29, 3.36, 3.43, 3.48, 3.55, 3.59, 3.66, 3.68, 3.89, 3.91, 3.94, 4.03, 4.10, <u>4.77</u> .
19	0+12p	0.12	<u>1.91</u> , 2.05, 2.42, 2.72, 2.74, 3.06, 3.13, 3.22, 3.89.
20	0+8p	0.58	<u>2.65</u> , 2.77, 3.25, 3.48, 3.71, 3.83, <u>5.23</u> .
21	0+14n	0.60	<u>2.12</u> , 2.21, 2.35, 2.88, 2.99, 3.20, 3.41, 3.48, 4.54, 4.72, 4.77, 4.88.
22	0+15p	25.19	<u>3.82</u> , 4.42, 4.60, 5.27, 5.48, 5.55, 5.64, 5.76, 5.78, 5.89, 5.92, 5.96, 6.01, 6.10, <u>6.15</u> .
23	0+16n	15.53	<u>3.22</u> , 3.68, 3.73, 3.91, 4.14, 4.65, 5.52, 5.73, 5.76, 5.96, 5.99, 6.22, 6.45, 6.47, 6.58.
24	0+15p	0.12	<u>0.30</u> , 0.94, 1.11, 1.96, 2.26, 2.69, 2.88, 3.11, 3.20, 3.32, 3.64, 3.87, 4.86, 5.34.
25	0+19n	0.48	<u>2.12</u> , 2.19, 2.42, 2.60, 2.86, 3.11, 3.22, 3.27, 3.41, 3.43, 3.45, 3.64, 3.85, 3.89, 4.19, 4.28, 4.54, 5.92.
26	0+11n	2.72	<u>2.69</u> , 2.92, 3.38, 3.48, 4.79, 4.83, 5.02, 5.23, 5.32, 5.64.

TABLE I (Continued)

Serial number	Event type	Primary energy (TeV)	Rapidity values
27	0+16p	0.54	<u>1.75</u> , 2.19, 2.26, 2.51, 2.51, 2.53, 2.84, 3.55, 3.62, 3.92, 4.56, 4.90, 5.11, 5.11, 5.55, <u>5.73</u> .
28	0+7n	1.04	<u>2.10</u> , 3.27, 3.41, 4.56, 4.72, 5.06, <u>5.78</u> .
29	0+17p	0.46	<u>1.01</u> , 1.47, 2.55, 2.81, 3.02, 3.02, 3.15, 3.20, 3.64, 3.96, 4.21, 4.47, 4.49, 4.54, 4.67, 4.81, <u>5.23</u> .
30	0+15p	0.19	<u>1.98</u> , 2.30, 2.37, 2.51, 2.55, 2.65, 2.74, 2.84, 2.99, 3.11, 3.22, 3.57, 4.49, 4.67, <u>4.95</u> .
31	0+2n	9402.09	<u>8.40</u> , <u>9.02</u> .
32	0+7p	2601.53	<u>7.12</u> , 7.21, 7.88, 7.90, 8.01, 8.47, <u>8.80</u> .
33	0+7n	6.69	<u>1.61</u> , 2.60, 5.76, 5.76, 6.27, 6.47, <u>6.65</u> .
34	0+13p	399.24	<u>1.45</u> , 4.67, 6.06, 6.79, 6.79, 7.02, 7.28, 7.71, 8.17, 8.17, 8.68, 9.10, <u>9.10</u> .
35	0+7p	0.91	<u>1.17</u> , 1.38, 2.21, 3.38, 7.18, 7.37, <u>7.51</u> .
36	0+13p	17.11	<u>2.21</u> , 3.52, 4.12, 5.37, 5.46, 5.50, 5.89, 6.01, 6.03, 6.10, 6.15, 6.63, <u>6.72</u> .
37	2+16p	4.1	<u>2.28</u> , 2.51, 3.11, 3.18, 3.20, 3.48, 3.96, 4.33, 5.50, 5.78, 5.94, 5.99, 6.22, 6.27, 6.36, <u>6.49</u> .
38	4+27p	5.7	<u>1.27</u> , 2.95, 3.09, 3.50, 3.64, 3.71, 3.82, 4.05, 4.14, 4.26, 4.70, 4.72, 4.77, 4.88, 4.95, 5.30, 5.30, 5.30, 5.41, 5.52, 5.80, 5.80, 5.99, 6.22, 6.22, 6.91, <u>7.18</u> .
39	0+20n	1.9	<u>0.51</u> , 1.15, 1.43, 1.98, 2.53, 3.36, 3.55, 4.33, 4.37, 4.42, 4.72, 4.93, 5.20, 5.25, 5.25, 5.39, 6.31, 6.40, 7.88, <u>12.90</u> .
40	2+15p	43.5	<u>2.49</u> , 2.99, 3.52, 3.64, 3.92, 4.31, 4.54, 4.58, 7.12, 7.12, 8.29, 8.29, 9.16, 9.90, <u>9.90</u> .
41	1+23p	2.1	<u>1.29</u> , 1.59, 1.59, 2.07, 2.21, 2.48, 2.48, 2.53, 3.13, 3.48, 3.48, 3.64, 4.00, 5.57, 5.71, 5.87, 5.87, 6.42, 6.90, 7.06, 7.13, 7.13, <u>7.18</u> .
42	3+32p	4.7	<u>2.48</u> , 2.58, 2.58, 2.90, 3.34, 3.34, 3.41, 3.50, 3.62, 3.73, 3.75, 3.80, 4.03, 4.19, 4.19, 4.35, 4.35, 4.37, 4.47, 4.56, 4.95, 5.64, 5.89, 5.89, 5.99, 6.10, 6.19, 6.27, 6.61, 7.81, 7.81, <u>8.52</u> .
43	0+20p	3.9	<u>0.53</u> , 1.59, 1.84, 1.93, 2.28, 2.86, 2.99, 3.89, 5.39, 5.66, 5.78, 5.80, 5.82, 6.10, 6.12, 6.29, 6.38, 6.49, 8.06, <u>8.06</u> .
44	0+13p	103.1	<u>2.42</u> , 2.86, 3.13, 3.34, 7.05, 7.05, 7.25, 7.32, 7.99, 7.99, 8.29, 8.98, <u>8.98</u> .
45	1+12p	3.4	<u>1.31</u> , 1.66, 2.28, 2.81, 3.50, 4.23, 6.19, 6.19, 6.88, 6.88, 6.88, <u>8.11</u> .
46	1+14p	2.2	<u>1.50</u> , 1.96, 2.19, 3.41, 3.76, 3.78, 4.05, 4.19, 5.50, 5.80, 6.10, 6.19, 6.42, <u>6.79</u> .
47	0+21n	0.4	<u>0.53</u> , 0.69, 1.20, 1.52, 1.57, 1.78, 2.03, 2.21, 2.39, 3.33, 3.73, 4.12, 4.88, 5.11, 5.11, 5.11, 5.11, 5.41, 5.50, 5.99, <u>6.17</u> .
48	2+20p	1.8	<u>1.77</u> , 1.89, 2.12, 2.21, 2.21, 2.99, 3.32, 3.78, 3.89, 3.89, 4.42, 4.69, 4.81, 5.11, 5.80, 5.80, 5.99, 6.49, 6.88, <u>6.88</u> .
49	2+23p	2.1	<u>1.29</u> , 1.59, 2.07, 2.23, 2.48, 2.53, 2.53, 3.11, 3.48, 3.64, 3.64, 4.05, 5.57, 5.73, 5.87, 5.87, 6.42, 7.04, 7.06, 7.06, 7.18, 7.18.
50	3+33p	1.6	<u>0.87</u> , 0.94, 1.15, 2.58, 2.70, 2.86, 3.20, 3.43, 3.48, 3.80, 3.82, 3.87, 3.89, 3.94, 4.05, 4.23, 4.23, 4.30, 4.37, 4.42, 4.47, 4.51, 4.69, 4.88, 4.88, 4.88, 5.30, 5.64, 5.80, 6.19, 6.19, 6.19, <u>6.65</u> .

TABLE I (Continued)

Serial number	Event type	Primary energy (TeV)	Rapidity values
51	4+26p	10.8	3.13, 3.15, 3.96, 4.10, 4.47, 4.56, 4.56, 4.58, 4.69, 4.69, 4.69, 4.81, 4.95, 4.95, 4.95, 5.30, 5.30, 5.50, 5.64, 5.80, 5.80, 6.19, 6.19, 6.49, 6.88, 6.88.
52	4+16p	1.4	0.87, 2.41, 2.72, 2.79, 2.90, 2.92, 3.09, 4.54, 4.69, 4.88, 5.30, 5.39, 5.46, 5.69, 6.40, 6.40.

diffractive components. We do not find any discontinuity in the Δ distribution plotted for all multiplicities. Hence it can be concluded that even at cosmic-ray energies the magnitude of Δ does not reflect the separate contributions from diffractive and nondiffractive dissociations. It is found that 13% of the events have $\Delta > 3.0$, and a large majority (80%) of such events have a multiplicity ≤ 13 and a primary energy greater than 1 TeV.

C. Rapidity-gap distribution

Snider³ has proposed a multiperipheral model which describes the two-charged-particle correlations and the rapidity-gap distribution for the

nondiffractive component of the hadronic cross section at high energies. Thus only the particles which constitute the central plateau have been considered, and the leading particles on each end in rapidity space have been neglected. This cut eliminates the contribution of a Pomeron at the ends of the rapidity distribution. Snider has obtained the following relation to compare with the experimental rapidity-gap distribution at 205 GeV/c p - p interactions. The relation is

$$\frac{dn}{dr} = 0.20e^{-0.9r} + 2.40e^{-3.1r}, \quad (5)$$

where r is the rapidity difference between neighboring charged particles.

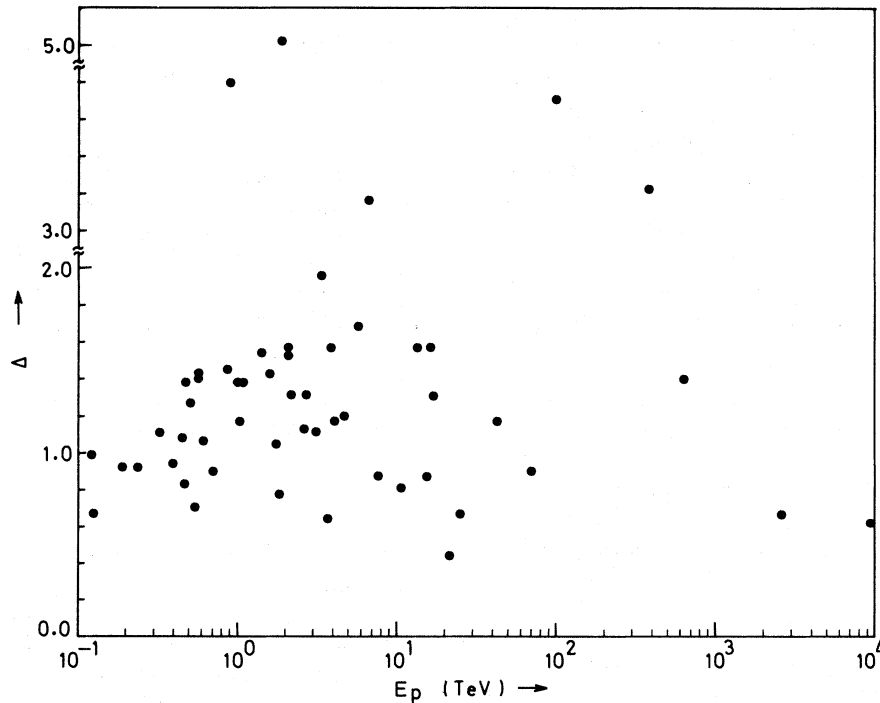


FIG. 1. Values of the maximum rapidity gap (Δ) versus the corresponding primary energy (E_p) of an interaction.

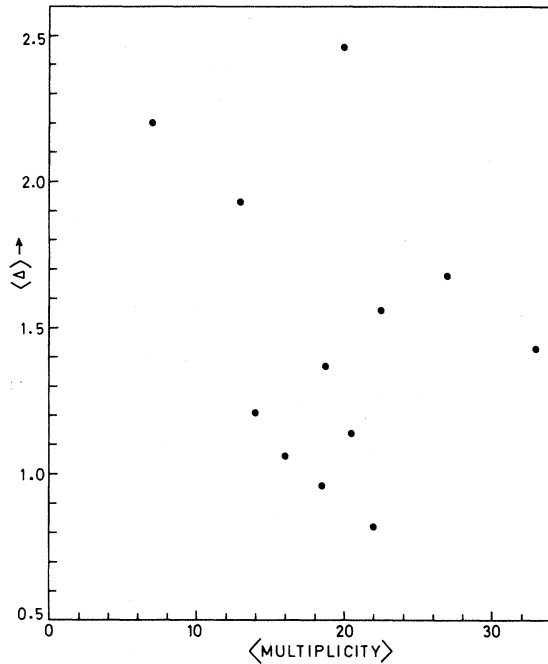


FIG. 2. Mean values of the maximum rapidity gap (Δ) versus the mean multiplicity.

We compare here the rapidity-gap distribution for p - p interactions at 205 GeV/ c with those at primary energies greater than 1 TeV. In the interactions under study the rapidity gap was calculated for all neighboring charged particles and the contribution of the two leading particles on each side of the rapidity distribution was neglected. Hence an event with multiplicity n contributed to the distribution $n - 3$ times. The rapidity-gap distribution thus obtained is for the central plateau of the rapidity distribution. Figure 3(a) shows the experimental and theoretical r distribution given by Snider,³ and Fig. 3(b) shows the r distribution obtained in the present work for $E_p > 1$ TeV. In Fig. 3(b) the solid curve represents the relation

$$\frac{dn}{dr} = 0.30e^{-1.0r} + 4.2e^{-5.1r}, \quad (6)$$

which is in agreement with the data well up to $r = 3.2$. From Eqs. (5) and (6) we see that the exponents of the first term (large r) in both equations are nearly the same, whereas there is a small difference in the values of the exponents in the second term (small r). The form of the distribution is nearly the same in both regions of primary energy [Figs. 3(a) and 3(b)]; this observation is in agreement with the predictions of the multiperipheral model. The multiperipheral model also predicts that the tail of the rapidity-gap distribution should be larger at very high energies.

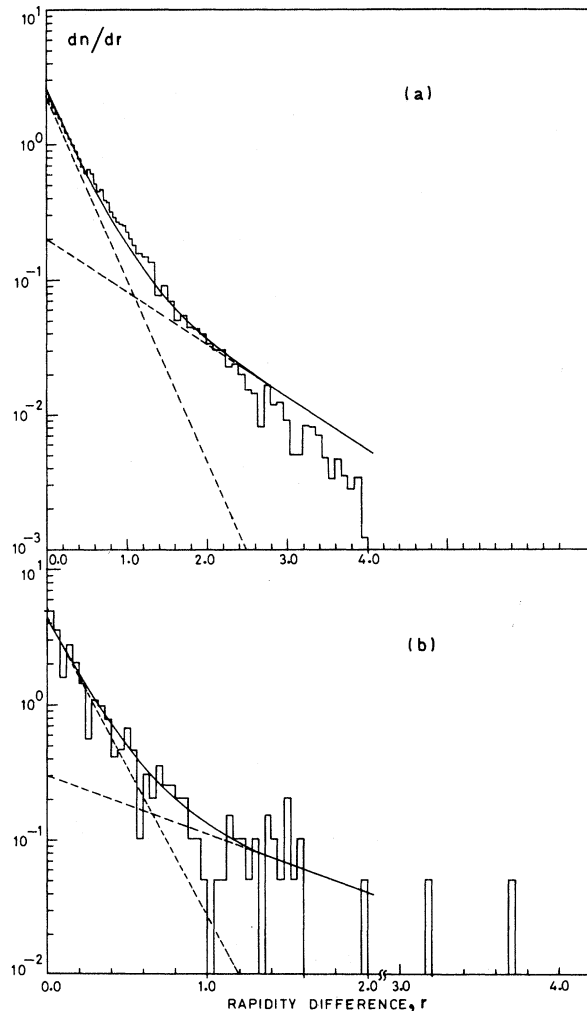


FIG. 3. Rapidity-gap distribution for neighboring charged particles in (a) 205 GeV/ c p - p collisions and (b) cosmic-ray interactions having a primary energy > 1.0 TeV. The solid curves in (a) and (b) show the respective contributions of Eqs. (5) and (6) in the text, and the dashed lines show the individual contributions of the two terms in the two equations.

The absence of such an observation in Fig. 3(b) is most likely due to low statistics in the present work.

D. Rapidity distribution

Using the multiperipheral concepts, viz. (a) that the transverse momenta are limited and (b) that the distant particles on the multiperipheral chain are uncorrelated, DeTar⁹ has explained the momentum spectrum of secondaries in a single-particle reaction of the type

$$a + b \rightarrow c + \text{anything.}$$

The observed logarithmic variation of charged-particle multiplicity with primary energy is clearly supported by the above model. Another prediction of the model is that the central region in the rapidity distribution is constant independent of the primary energy. Writing the total cross section as σ_{ab} and g^2 to correspond to that vertex which emits the type of particle under consideration, $d\sigma_{ab}/dy$ can be expressed as shown by DeTar⁹

$$\frac{d\sigma_{ab}(Y-y)}{dy} = e^{-Y} B_a(y) g^2 B_b(Y-y).$$

The form of the y distribution is thus rectangular in shape; the width varies as a function of the primary energy. This is clearly in agreement with the experimental data, as seen from Fig. 4, which shows the laboratory rapidity distribution of the secondaries (excluding the persisting primary) which are mostly pions. The events considered in Fig. 4 have E_p ranging from 0.1 to 2600.0 TeV, and have $n_h = 0$. Figures 4(a) and 4(b) show the rapidity distribution for events having a primary energy greater than 1 TeV and less than 1 TeV, respectively. The choice of grouping the events as in

Figs. 4(a) and 4(b) is dictated by the nearly equal number of tracks in the two energy ranges. It is seen from Figs. 4(a) and 4(b) that the height of the rapidity distribution at the center is constant independent of the primary energy. With the increase in primary energy, the central plateau of the distribution is shifted towards the higher region of the rapidity spectrum. The distribution at the center is due to the particles that decouple from the distant particles of the multiperipheral chain and hence must be independent of both target and beam. The shape at the ends of Figs. 4(a) and 4(b) is due to the particles produced at the ends of the chain which are dynamically uncorrelated with particles produced elsewhere in the chain. Thus we find that the observed rapidity spectrum is well explained on the basis of the multiperipheral model.

ACKNOWLEDGMENT

We are very grateful to Professor Dale R. Snider for sending us data on rapidity differences in 205-GeV/c p - p interactions.

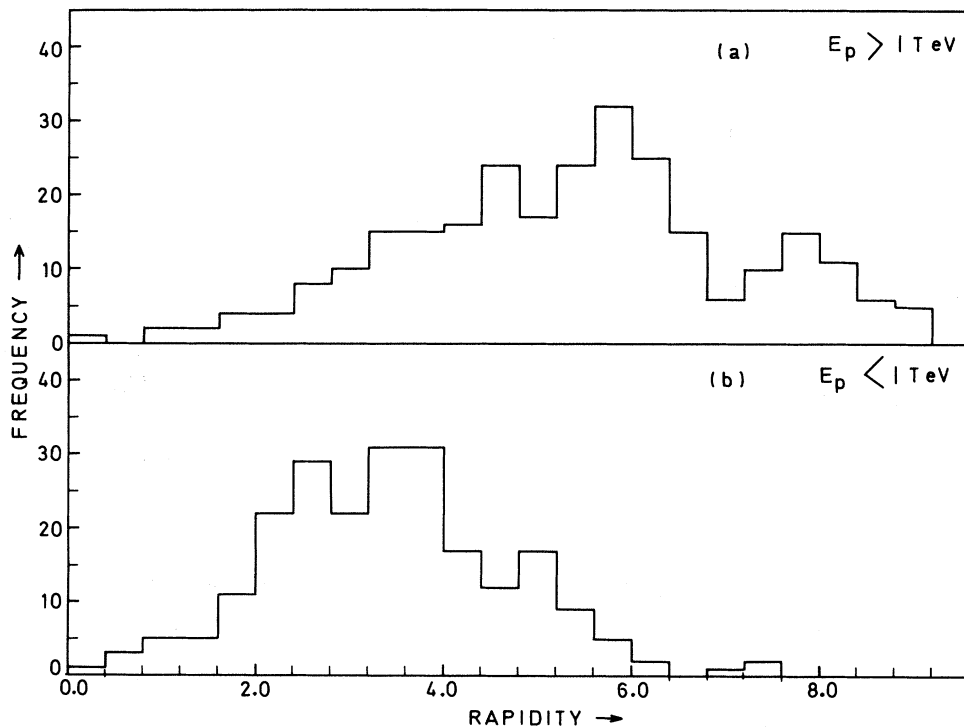


FIG. 4. Rapidity distribution of secondary particles for events having a primary energy (E_p) (a) >1.0 TeV and (b) <1.0 TeV, respectively.

- ¹R. P. Feynman, Phys. Rev. Lett. 23, 1415 (1969); in *High Energy Collisions*, proceedings of the Third International Conference, Stony Brook, 1969, edited by C. N. Yang *et al.* (Gordon and Breach, New York, 1969), p. 237.
- ²S. T. Jones and D. R. Snider, Phys. Rev. D 9, 242 (1974).
- ³Dale R. Snider, Phys. Rev. D 11, 140 (1975).
- ⁴I.C.E.F. Collaboration, Nuovo Cimento Suppl. 1, 1039 (1963).
- ⁵Following the usual nomenclature, tracks having ionization >1.4 times the minimum are termed heavy tracks (n_h) and those having ionization ≤ 1.4 times the minimum are called shower tracks (n_s). The former are due to knock-on nucleons and the evaporation of nuclei, and the latter are due to elementary nucleon-nucleon collisions.
- ⁶A. G. Barkow, B. Chamany, D. M. Haskin, P. L. Jain, E. Lohrmann, M. W. Teucher, and M. Schein, Phys. Rev. 122, 617 (1961); M. Schein, D. Haskin, E. Lohrmann, and M. W. Teucher, *ibid.* 116, 1238 (1959).
- ⁷C. Castagnoli, G. Cortini, D. Moreno, C. Franzinetti, and A. Manfredini, Nuovo Cimento 10, 1539 (1. 53).
- ⁸B. Bhowmik and R. K. Shivpuri, Can. J. Phys. 47, 195 (1969).
- ⁹Carlton E. DeTar, Phys. Rev. D 3, 128 (1971).